

Silicon Self-Diffusion in Isotope Heterostructures

H. Bracht and E. E. Haller

University of California at Berkeley and Lawrence Berkeley National Laboratory, Berkeley, California 94720

R. Clark-Phelps

Charles Evans & Associates, 301 Chesapeake Drive, Redwood City, 94063

(Received 9 February 1998)

Self-diffusion of silicon is measured between 855 and 1388 °C in highly isotopically enriched ^{28}Si layers. The profiles of ^{29}Si and ^{30}Si are determined by secondary ion mass spectrometry. Temperature dependence of the self-diffusion coefficients is accurately described over seven orders of magnitude with one diffusion enthalpy of 4.75 eV. This single enthalpy indicates that self-interstitials dominate self-diffusion. The high accuracy of our data enables us to estimate an upper bound for the vacancy-assisted diffusion enthalpy of 4.14 eV, which agrees with recent theoretical calculations. [S0031-9007(98)06537-5]

PACS numbers: 66.30.Hs, 61.72.Ji

Self-diffusion in a homogeneous solid is a fundamental process of matter transport [1]. Optimal media for self-diffusion studies are chemically pure and structurally perfected single crystals of semiconductors. The native defects—such as vacancies and self-interstitials—have been established as the prime entities controlling the self-diffusion as well as the diffusion of impurities in semiconductor lattices. Diffusion is essential for semiconductor device technology, yet the present qualitative and quantitative understanding of the physics of diffusion in Si is far from satisfactory [2,3]. This paper reports self-diffusion in Si with one layer of the highly enriched isotope ^{28}Si incorporated in a heterostructure, which otherwise represents a homogeneous Si sample. Secondary ion mass spectrometry (SIMS) with high spatial resolution yields new information, revealing that self-interstitials dominate self-diffusion over a wide temperature range.

Silicon self-diffusion experiments were carried out using the radiotracer ^{31}Si with a half-life of about 2.6 h [4–7]. However, this short-lived radiotracer limits such studies to a narrow high-temperature range near the melting point $T_m = 1412$ °C. Other self-diffusion experiments utilizing the stable isotope ^{30}Si in conjunction with neutron activation analysis [8], SIMS [9,10], and the $^{30}\text{Si}(p, \gamma)^{31}\text{Si}$ resonance broadening method [11,12] overcame this difficulty. These methods, however, have the disadvantage that the ^{30}Si background concentration in natural Si is high (3.10%). More accurate Si self-diffusion data over a wide temperature range are not only of interest in modeling complex processing steps but are also most relevant for the understanding of the individual contributions of the various native defects, foremost interstitials, and vacancies. The self-diffusion activation energies reported so far all lie in the narrow energy range of 4 to 5 eV [2]. Combining the low- and high-temperature data a “kink” in the Arrhenius plot of Si self-diffusion was generally supposed. Only accurate self-diffusion experi-

ments over a wide temperature range may resolve whether such a kink really exists. Recent calculations of the properties of native point defects in Si have been considerably improved [14–17]. Therefore reliable experiments are required for quantitative comparison.

Compared to earlier experiments, Si self-diffusion can be studied over a wide temperature range in greater detail with isotopically controlled Si heterostructures at internal interfaces. Isotope heterostructures have already been used for investigating Ge self-diffusion [18] and Ga self-diffusion both in GaAs [19] and GaP [20]. The main advantage of experiments with isotope heterostructures is the extension to a wider temperature range. We therefore can determine directly for the first time whether the mechanism of self-diffusion changes with decreasing temperature. In general, taking into account all contributions, the self-diffusion coefficient is given by

$$D^{\text{SD}} = f_I C_I^{\text{eq}} D_I + f_V C_V^{\text{eq}} D_V + D_{\text{exchange}}. \quad (1)$$

The first two terms represent the self-interstitial (I) and the vacancy (V) contribution to self-diffusion, where $C_{I,V}^{\text{eq}}$ and $D_{I,V}$ are the equilibrium concentrations in atomic fractions (unitless) and diffusion coefficients of I and V ; $f_{I,V}$ are the correlation factors for the corresponding diffusion mechanism, which were calculated to be $f_I \approx 0.73$ [21] and $f_V = 0.5$ [22] for the interstitialcy and the vacancy mechanism in the diamond lattice. The last term accounts for a direct exchange of adjacent lattice atoms. This contribution will not be considered for Si self-diffusion, because calculations have shown that it does not play a role [14–16]; no experimental evidence has been found for it.

Our Si self-diffusion experiments used four different Si-isotope heterostructures which were grown by chemical vapor deposition at about 900 °C on natural floating-zone Si substrates. Heterostructure No. 1 consists of a 5 μm thick p -type ^{28}Si layer grown on p -type substrate.

The boron concentration of the ^{28}Si epilayer and the substrate was determined by SIMS to be $<10^{15} \text{ cm}^{-3}$ and $5 \times 10^{18} \text{ cm}^{-3}$, respectively. The isotope heterostructure No. 2 consists of a $5 \mu\text{m}$ thick n -type ^{28}Si layer grown on p -type natural Si substrate. The phosphorus (P) and boron (B) concentrations in the epilayer and the substrate of this structure are about 3×10^{15} and $4 \times 10^{15} \text{ cm}^{-3}$, respectively. In addition to these samples, a 400 nm thick B-doped ($[\text{B}] = 4 \times 10^{18} \text{ cm}^{-3}$, heterostructure No. 3) and a 500 nm thick P-doped ($[\text{P}] \leq 2 \times 10^{18} \text{ cm}^{-3}$, heterostructure No. 4) ^{28}Si layer were grown on natural Si substrates with B and P concentrations of 10^{19} cm^{-3} and about 10^{16} cm^{-3} , respectively. In contrast to the isotope heterostructures No. 1 and No. 2, structures No. 3 and No. 4 are covered with a natural Si layer of about 200 nm thickness which are doped equally to the underlying isotopically enriched ^{28}Si layer. The isotope composition in all enriched ^{28}Si epilayers was determined by SIMS to be $^{28}\text{Si}:^{29}\text{Si}:^{30}\text{Si} = 99.92:0.078:0.002$ (natural Si:92.2:4.7:3.1). SIMS analysis yields an oxygen concentration of $2 \times 10^{17} \text{ cm}^{-3}$ and a carbon concentration of $7 \times 10^{15} \text{ cm}^{-3}$ in the heterostructures.

Samples of $5 \times 5 \text{ mm}^2$ lateral dimensions were sealed in quartz ampoules under pure argon (99.999%) atmosphere. Diffusion experiments were performed in resistance furnaces. The temperature was monitored with an accuracy of $\pm 2 \text{ K}$ with a calibrated Pt/PtRh thermocouple contacting the ampoule. After annealing, the distribution of ^{29}Si and ^{30}Si in the ^{28}Si epilayer was measured with SIMS. This analysis was performed with a double-focusing magnetic sector mass spectrometer (CAMECA IMS-3f) using a Cs^+ ion-beam energy of either 14.5 or 5.5 keV . A quadrupole mass spectrometer (PHI 6650) with a primary beam of 3 keV Cs^+ ions was used when a better depth resolution was necessary. Crater depths were measured with a Tencor P-10 surface profilometer with an accuracy of 10%.

Heterostructures No. 1 and No. 2 were used at temperatures between 1388 and $1020 \text{ }^\circ\text{C}$. Concentration profiles of ^{30}Si near the interface of the ^{28}Si epilayer and the natural Si substrate of heterostructure No. 2 and two samples annealed at 1095 and $1153 \text{ }^\circ\text{C}$ are shown in Fig. 1. The solid lines show best fits of experimental profiles which are based on

$$C(x) = \frac{C_1 + C_2}{2} + \frac{C_1 - C_2}{2} \operatorname{erf}\left(\frac{x - d_1}{R}\right) \quad (2)$$

being the solution of Fick's law for self-diffusion across an interface. C_1 and C_2 are the concentrations of ^{30}Si in the natural Si substrate and the ^{28}Si epilayer, respectively. The thickness of the isotope epilayer is denoted as d_1 ; R represents the characteristic diffusion length $R = 2(D_{\text{Si}}^{\text{SD}} t)^{0.5}$, and t is the annealing time. Si profiles are not affected by instrumental broadening caused by SIMS sputtering effects, as has been checked by a deconvolution routine [23].

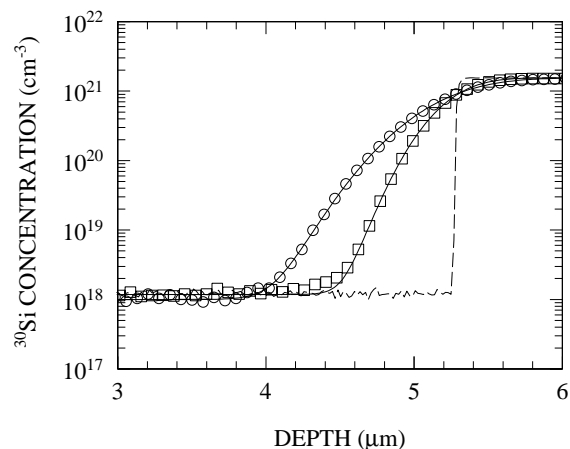


FIG. 1. SIMS depth profiles of ^{30}Si measured before (dashed line) and after annealing at $1095 \text{ }^\circ\text{C}$ (\square , $t = 54.5 \text{ h}$) and $1153 \text{ }^\circ\text{C}$ (\circ , $t = 19.5 \text{ h}$) of the ^{28}Si isotope heterostructure No. 2. For clarity only every fourth experimental data point is plotted. Solid lines show best fits to the experimental data.

Heterostructures No. 3 and No. 4 were used between 1020 and $855 \text{ }^\circ\text{C}$. Assuming a step function for both interfaces in the as-grown structure, experimental profiles measured after annealing at temperatures between 1020 and $940 \text{ }^\circ\text{C}$ were fitted with

$$C(x) = \frac{C_1 + C_3}{2} + \frac{C_2 - C_3}{2} \operatorname{erf}\left(\frac{x - d_2}{R}\right) + \frac{C_1 - C_2}{2} \operatorname{erf}\left(\frac{x - d_1 - d_2}{R}\right) \quad (3)$$

using R as fitting parameter. Here C_3 is the concentration of ^{30}Si in the natural Si top layer with thickness d_2 . The meaning of the other parameters is as given for Eq. (2). Si profiles measured after annealing at 855 , 880 , and $911 \text{ }^\circ\text{C}$ were fitted by solving Fick's law for self-diffusion numerically. In this case, we have taken into account the measured as-grown profile of No. 3 and No. 4 as initial solution, because SIMS analysis with improved depth resolution has revealed that the as-grown Si profile is already broadened by self-diffusion during the growth and not by SIMS sputtering effects. For temperatures above $911 \text{ }^\circ\text{C}$, Si self-diffusion was more pronounced; the length R was accurately extracted by fitting Eq. (3) to the experimental profiles.

Self-diffusion coefficients $D_{\text{Si}}^{\text{SD}}$ obtained from the analysis of all experiments performed between 1388 and $855 \text{ }^\circ\text{C}$ are presented in Fig. 2. The experimental error for $D_{\text{Si}}^{\text{SD}}$ was estimated to lie between 20% and 25% and is mainly caused by the accuracy of the depth measurement of the craters left from the SIMS sputtering. Values for $D_{\text{Si}}^{\text{SD}}$ span seven orders of magnitude within the temperature range investigated and are accurately described by an Arrhenius equation with one single activation enthalpy

$$D_{\text{Si}}^{\text{SD}} = (530_{-170}^{+250}) \exp\left(-\frac{(4.75 \pm 0.04)\text{eV}}{k_B T}\right) \text{ cm}^2 \text{ s}^{-1}. \quad (4)$$

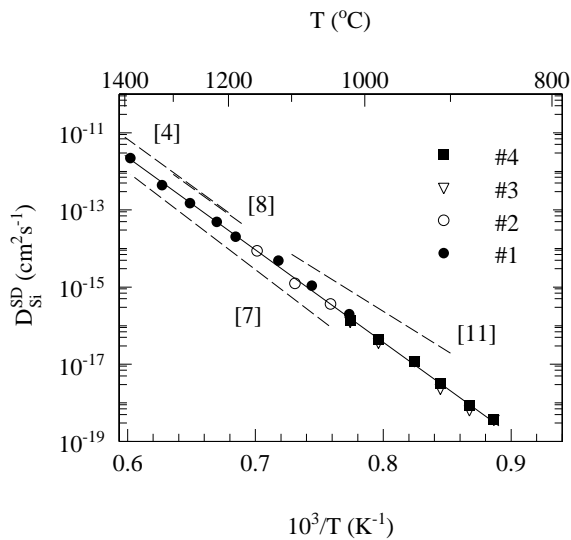


FIG. 2. Temperature dependence of the Si self-diffusion coefficient $D_{\text{Si}}^{\text{SD}}$ obtained from our self-diffusion study with isotope heterostructures (symbols, solid line) in comparison to literature data (dashed line) with reference numbers shown in brackets.

Analysis of ^{29}Si diffusion profiles which were recorded together with the distribution of ^{30}Si yields data for $D_{\text{Si}}^{\text{SD}}$ which are consistent within 10% or better with the results shown in Fig. 2. The temperature dependence of $D_{\text{Si}}^{\text{SD}}$ data deduced from ^{29}Si profiles yields the same preexponential factor and activation enthalpy of self-diffusion as given by Eq. (4). Self-diffusion data given by Fairfield and Masters [5,6] for temperatures between 1100 and 1300 °C and our results for this range are consistent. For temperatures lower than 1200 °C, $D_{\text{Si}}^{\text{SD}}$ values reported by Kalinowski and Seguin [9,10] and by Demond *et al.* [12] agree well with our values. However, the temperature dependence of the Si self-diffusion reported by these authors is described by an activation enthalpy of $H^{\text{SD}} = 5.13$ eV for high temperatures [5,6] and of $H^{\text{SD}} = 4.65$ eV [9,10] and $H^{\text{SD}} = 4.4$ eV [12] for low temperatures. Based on these earlier findings, it was assumed that the mechanism of Si self-diffusion changes when going from high to low temperatures. In contrast to this generally accepted view, the temperature dependence of our results for $D_{\text{Si}}^{\text{SD}}$ clearly indicates that only one diffusion mechanism dominates Si self-diffusion in this temperature range. The native defect mediating self-diffusion is considered to be the self-interstitial. This conclusion is consistent with experimental data for $C_I^{\text{eq}} D_I$ (see below) and recent calculations [16].

The thermal equilibrium concentration C_I^{eq} of self-interstitials and their diffusivity D_I are described by

$$C_I^{\text{eq}} = C_0 \exp(S_I^f/k_B) \exp(-H_I^f/k_B T), \quad (5)$$

$$D_i = g a_0^2 \nu_0 \exp(S_I^m/k_B) \exp(-H_I^m/k_B T), \quad (6)$$

where H_I^f and H_I^m , respectively, are the formation and migration enthalpies and $S_I^{f,m}$ denotes the respective entropy. $C_0 = 5 \times 10^{22} \text{ cm}^{-3}$ is the Si atom density, $a_0 =$

$5.431 \times 10^{-8} \text{ cm}$ the jump distance, $g = 1/4$ the geometry factor for the interstitialcy mechanism [24], and ν_0 an attempt frequency, which is estimated as the Debye frequency of $\sim 10^{13} \text{ s}^{-1}$. According to Eqs. (4)–(6), the activation enthalpy $H_I^{\text{SD}} = H_I^f + H_I^m$ of I -mediated self-diffusion is 4.75 eV. The corresponding entropy $S_I^{\text{SD}} = S_I^f + S_I^m = (11.5 \pm 0.4)k_B$ was calculated from the preexponential factor of Eq. (4). A recent calculation by Tang *et al.* [17] of $H_I^{\text{SD}} = (5.13 \pm 0.2) \text{ eV}$ yields a slightly higher value than our experimental finding. As shown below, this difference is considered as an indication of a small contribution of vacancies in Si self-diffusion contained in the temperature dependence of $D_{\text{Si}}^{\text{SD}}$.

Doping exerts no observable effects, even at our lowest temperatures. Self-diffusion is therefore considered to occur under intrinsic conditions. After annealing at 855 °C, the P concentration of heterostructure No. 4 was determined to be 10^{18} cm^{-3} . This concentration is below the intrinsic carrier concentration $n_i(855 \text{ °C}) = 3.5 \times 10^{18} \text{ cm}^{-3}$ [25], and therefore no change in $D_{\text{Si}}^{\text{SD}}$ due to the Fermi-level position is expected. The B concentration of material No. 3 after annealing at 855 °C was measured to be $6 \times 10^{18} \text{ cm}^{-3}$. This doping level exceeds the intrinsic carrier concentration. The influence of B doping on $C_I^{\text{eq}} D_I$ was recently deduced from Au diffusion experiments into heavily B-doped Si samples [26]. Based on these results, $C_I^{\text{eq}} D_I$ at 855 °C is expected to increase by about (20–25)% for a B concentration of $6 \times 10^{18} \text{ cm}^{-3}$. Therefore, the effect of the Fermi level on $D_{\text{Si}}^{\text{SD}}$ lies within our experimental error for $D_{\text{Si}}^{\text{SD}}$ and cannot be expected to be resolved. If we ignore data for $D_{\text{Si}}^{\text{SD}}$ deduced from the annealed B-doped isotope structures, we obtain a preexponential factor of $430 \text{ cm}^2 \text{ s}^{-1}$ and an activation enthalpy of 4.72 eV. These values lie within the standard deviation of these quantities which are obtained if all $D_{\text{Si}}^{\text{SD}}$ data were taken into account [see Eq. (4)].

Results from self-diffusion studies are generally not easily separable into the individual contributions given on the right-hand side of Eq. (1). However, since the contribution $C_I^{\text{eq}} D_I$ of self-interstitials to Si self-diffusion is already well known from metal diffusion experiments in Si [27,28], we can extract data for $C_V^{\text{eq}} D_V$ from our self-diffusion data. Taking into account

$$C_I^{\text{eq}} D_I = 2980 \exp(-4.95 \text{ eV}/k_B T) \text{ cm}^2 \text{ s}^{-1} \quad (7)$$

which was obtained from the analysis of Zn diffusion into Si [28], the best fit of our experimental $D_{\text{Si}}^{\text{SD}}$ data on the basis of Eq. (1) assuming $D_{\text{exchange}} \approx 0$ is obtained with

$$C_V^{\text{eq}} D_V = 0.92 \exp(-4.14 \text{ eV}/k_B T) \text{ cm}^2 \text{ s}^{-1}. \quad (8)$$

Equations (7) and (8) reveal that $C_I^{\text{eq}} D_I$ equals $C_V^{\text{eq}} D_V$ at about 890 °C and not at temperatures between 1000 and 1100 °C as it has been generally assumed. The estimate for $C_V^{\text{eq}} D_V (= 0.6 \exp(-4.03/k_B T) \text{ cm}^2 \text{ s}^{-1})$ given by Tan and Gsele [29], based on the analysis of metal diffusion experiments, does not deviate much from our

result. The activation enthalpy of self-diffusion H^{SD} for self-interstitials and vacancies which were found to accurately describe our self-diffusion data are $H_I^{\text{SD}} = 4.95$ eV and $H_V^{\text{SD}} = 4.14$ eV. These results are in excellent agreement with recent tight-binding molecular dynamic studies which yield $H_I^{\text{SD}} = (5.18 \pm 0.2)$ eV and $H_V^{\text{SD}} = (4.07 \pm 0.2)$ eV [17]. The entropy of I -mediated self-diffusion $S_I^{\text{SD}} = 13.2k_B$ calculated from Eq. (7) is also in very good agreement with $S_I^{\text{SD}} = 14.3k_B$ given by Tang *et al.* [17]. According to Eq. (8) and equations for vacancies similar to Eqs. (5) and (6), $S_V^{\text{SD}} (= S_V^f + S_V^m)$ is found to be $5.5k_B$. Calculations of the V -related formation entropy yield $S_V^f = (5 \pm 2)k_B$ [16]. Therefore, the migration entropy S_V^m , which has not yet been calculated accurately, is expected to lie within $1k_B$ to $2k_B$.

In conclusion, we have studied Si self-diffusion with isotopically controlled heterostructures. The temperature dependence of self-diffusion was found to be dominated by a single activation enthalpy of 4.75 eV. Taking into account the highly reliable experimental data for $C_I^{\text{eq}}D_I$, the vacancy contribution to self-diffusion is obtained showing that self-interstitials dominate self-diffusion almost over the entire temperature range investigated which is consistent with recent first principles calculations [16]. Comparison of the activation enthalpy and entropy of I - and V -mediated self-diffusion obtained from our self-diffusion study and calculations reveal very good agreement between experiment and theory.

One of us (H. B.) gratefully acknowledges support by the Alexander von Humboldt-Stiftung. We are grateful to ISONICS Corp. for providing the highly enriched ^{28}Si and to Professor H.-J. Queisser for critically reviewing the manuscript. This work was supported in part by the Director, Office of Energy Research, Office of Basic Energy Sciences, Materials Sciences Division of the U.S. Department of Energy under Contract No. DE-AC03-76SF00098 and in part by U.S. NSF Grant No. DMR-94 17763.

-
- [1] A. C. Damask and G. J. Dienes, *Point Defects in Metals* (Gordon and Breach, New York, 1963).
 - [2] W. Frank, U. Gösele, H. Mehrer, and A. Seeger, in *Diffusion in Crystalline Solids*, edited by G. E. Murch and A. S. Nowick (Academic, New York, 1984).
 - [3] P. M. Fahey, P. B. Griffin, and J. D. Plummer, *Rev. Mod. Phys.* **61**, 289 (1989).

- [4] R. F. Peart, *Phys. Status Solidi* **15**, K119 (1966).
- [5] B. J. Masters and J. M. Fairfield, *Appl. Phys. Lett.* **8**, 280 (1966).
- [6] J. M. Fairfield and B. J. Masters, *J. Appl. Phys.* **38**, 3148 (1967).
- [7] H. J. Mayer, H. Mehrer, and K. Maier, in *Proceedings of the IOF International Conference on Radiation Effects in Semiconductors, Dubrovnik, 1976* (Institute of Physics, London, 1977), p. 186.
- [8] R. N. Ghoshtagore, *Phys. Rev. Lett.* **16**, 890 (1966).
- [9] L. Kalinowski and R. Seguin, *Appl. Phys. Lett.* **35**, 211 (1979).
- [10] L. Kalinowski and R. Seguin, *Appl. Phys. Lett.* **36**, 171 (1980).
- [11] J. Hirvonen and A. Anttila, *Appl. Phys. Lett.* **35**, 703 (1979).
- [12] F. J. Demond, S. Kalbitzer, H. Mannsperger, and H. Damjantschitsch, *Phys. Lett.* **93A**, 503 (1983).
- [13] *Diffusion in Solids Metals and Alloys*, edited by H. Mehrer, Landolt-Börnstein, New Series, Group III, Vol. 26 (Springer, Berlin, 1990).
- [14] K. C. Pandey, *Phys. Rev. Lett.* **57**, 2287 (1986).
- [15] K. C. Pandey and E. Kaxiras, *Phys. Rev. Lett.* **66**, 915 (1990).
- [16] P. E. Blöchl, E. Smargiassi, R. Car, D. B. Laks, W. Andreoni, and S. T. Pantelides, *Phys. Rev. Lett.* **70**, 2435 (1993).
- [17] M. Tang, L. Colombo, J. Zhu, and T. Diaz de la Rubia, *Phys. Rev. B* **55**, 14 279 (1997).
- [18] H. D. Fuchs, W. Walukiewicz, E. E. Haller, W. Dondl, R. Schorer, G. Abstreiter, A. I. Rudnev, A. V. Tikhomirov, and V. I. Ozogin, *Phys. Rev. B* **51**, 16 817 (1995).
- [19] L. Wang, L. Hsu, E. E. Haller, J. W. Erickson, A. Fischer, K. Eberl, and M. Cardona, *Phys. Rev. Lett.* **76**, 2342 (1996).
- [20] L. Wang, J. A. Wolk, L. Hsu, E. E. Haller, J. W. Erickson, M. Cardona, T. Ruf, J. P. Silveira, and F. Briones, *Appl. Phys. Lett.* **70**, 1831 (1997).
- [21] K. Compaan and Y. Haven, *Trans. Faraday Soc.* **54**, 1498 (1958).
- [22] K. Compaan and Y. Haven, *Trans. Faraday Soc.* **52**, 786 (1956).
- [23] P. S. Ho and J. E. Lewis, *Surf. Sci.* **55**, 335 (1976).
- [24] A. Seeger, H. Föll, and W. Frank, in Ref. [7], p. 12.
- [25] F. J. Morin and J. P. Maita, *Phys. Rev.* **96**, 28 (1954).
- [26] H. Bracht, *Diffusion and Defect Forum* **143-147**, 979 (1997).
- [27] N. A. Stolwijk, B. Schuster, J. Hölzl, H. Mehrer, and W. Frank, *Physica (Amsterdam)* **116B&C**, 335 (1983).
- [28] H. Bracht, N. A. Stolwijk, and H. Mehrer, *Phys. Rev. B* **52**, 16 542 (1995).
- [29] T. Y. Tan and U. Gösele, *Appl. Phys. A* **37**, 1 (1985).